Bioelectrochemistry 121 (2018) 142–150

Contents lists available at ScienceDirect

Bioelectrochemistry

journal homepage: www.elsevier.com/locate/bioelechem

Simultaneous measurements of ascorbate and glutamate *in vivo* in the rat brain using carbon fiber nanocomposite sensors and microbiosensor arrays

Nuno R. Ferreira [a], Ana Ledo [b], João Laranjinha [a,b], Greg A. Gerhardt [c], Rui M. Barbosa [a,b,*]

[a] Faculty of Pharmacy, University of Coimbra, 3000-548 Coimbra, Portugal
[b] Center for Neuroscience and Cell Biology, University of Coimbra, 3004-517 Coimbra, Portugal
[c] Department of Neuroscience, Center for Microelectrode Technology, University of Kentucky, Lexington, USA

ARTICLE INFO

Article history:
Received 15 December 2017
Received in revised form 15 January 2018
Accepted 19 January 2018
Available online 31 January 2018

Keywords:
Ascorbate
Glutamate
Carbon nanotubes
Microelectrode arrays
In vivo monitoring

ABSTRACT

Nanocomposite sensors consisting of carbon fiber microelectrodes modified with Nafion® and carbon nanotubes, and ceramic-based microelectrode biosensor arrays were used to measure ascorbate and glutamate in the brain with high spatial, temporal and chemical resolution. Nanocomposite sensors displayed electrocatalytic properties towards ascorbate oxidation, translated into a negative shift from +0.20 V to −0.05 V *vs.* Ag/AgCl, as well as a significant increase (10-fold) of electroactive surface area. The estimated average basal concentration of ascorbate *in vivo* in the CA1, CA3 and *dentate gyrus* (DG) sub regions of the hippocampus were 276 ± 60 μM (n = 10), 183 ± 30 μM (n = 10) and 133 ± 42 μM (n = 10), respectively. The glutamate microbiosensor arrays showed a high sensitivity of 5.3 ± 0.8 pA μM^{-1} (n = 18), and LOD of 204 ± 32 nM (n = 10), and $t_{50\%}$ response time of 0.9 ± 0.02 s (n = 6) and high selectivity against major interferents. The simultaneous and real-time measurements of glutamate and ascorbate in the hippocampus of anesthetized rats following local stimulus with KCl or glutamate revealed a dynamic interaction between the two neurochemicals.

1. Introduction

Ascorbate plays important roles in the neurophysiological processes of the brain, ranging from antioxidant and enzyme co-factor to a modulator of energetic metabolism as well as glutamate and nitric oxide (•NO) dependent signaling processes [1,2]. Glutamate is the major excitatory neurotransmitter in the mammalian central nervous system and is key to glia-neuron communication [3] and brain functions such as cognition, memory and learning. It has been suggested that changes in extracellular glutamate levels are coupled to fluctuations in extracellular ascorbate levels *via* a hetero-exchange mechanism involving glutamate transporters [4,5], in a process mediated by •NO produced upon activation of NMDA-type glutamate receptors [2]. Interestingly, deregulation in both glutamate- and ascorbate-dependent pathways appear to play a role in neurodegenerative processes such as Alzheimer's or Huntington's disease [6–9]. The monitoring of both compounds *in vivo* with high spatial and temporal resolution may offer new insights into the dynamic interplay between these two neurochemicals during excitatory neurotransmission.

Carbon nanotubes (CNTs) have been widely used for the fabrication of electrochemical sensors and biosensors owing to their unique structural, mechanical, chemical and electronic properties which offer several advantages, namely high surface-to-volume ratios, promotion of electron transfer reactions, decrease of over-potentials for various electroactive compounds, increase in sensitivity and reduction of surface fouling [10–12]. Due to their electrocatalytic properties, CNT composite films have been used to modify the surface of carbon fiber microelectrodes (CFM) for *in vivo* measurements of ascorbate in the rat brain [13,14].

Glutamate is commonly monitored *in vivo* by microdialysis [15], which allows the identification of relevant chemicals by using powerful analytical techniques such as HPLC-ECD or LC-MS-MS. However, this approach presents limitations such as the significant damage to brain tissue due to probe size that ranges between 150 and 500 μm in diameter and 1–4 mm in length [16–18], lack of spatial resolution of microdialysis probes [15], and inadequate temporal resolution to detect rapid synaptic-related events. An attractive alternate approach encompasses the use of ceramic microelectrode arrays (MEAs) coated with glutamate oxidase (GluOx) coupled to fast electrochemical techniques such as amperometry to monitor glutamate in the brain extracellular space [19,20]. These microbiosensor arrays have been successfully used for second-by-second measures, in a self-referencing mode, of tonic and potassium-evoked glutamate levels in anesthetized rodents [21,22] as

* Corresponding author at: Faculdade de Farmácia, Universidade de Coimbra, Polo das Ciências da Saúde, Azinhaga de Santa Comba, 3000-548 Coimbra, Portugal.
E-mail address: rbarbosa@ff.uc.pt (R.M. Barbosa).

https://doi.org/10.1016/j.bioelechem.2018.01.009
1567-5394/

well as tonic and evoked changes in chronic recordings in freely moving animals [23].

In this work, we have characterized the electrocatalytic oxidation of ascorbate at CFMs coated with different CNT composite films, which increased the electrochemical active surface area. These nanocomposite sensors were used for the measurement of basal levels of ascorbate in the CA1, CA3 and *dentate gyrus* (DG) sub regions of the hippocampus of urethane anesthetized rats. Moreover, the kinetic and analytical performance of the glutamate microbiosensor array was assessed *in vitro* and they were used to characterize glutamate dynamics upon potassium stimulation in the brain of anesthetized rats. Finally, the two micro(bio)sensors were assembled in an array and used for simultaneous measurement of ascorbate and glutamate *in vivo* to assess the dynamic interplay between these two neurochemicals with high spatial and temporal resolution.

2. Experimental

2.1. Reagents and solutions

Ascorbate and *o*-phenylenediamine (*o*-PD) were obtained from Fluka. KCl was obtained from Panreac (Barcelona, Spain). All other reagents were analytical grade and obtained from Sigma-Aldrich, unless otherwise stated. Phosphate buffered saline (0.05 M PBS) used for microelectrodes evaluations was prepared in Milli-Q water and had the following composition (mM): 10 NaH_2PO_4, 40 Na_2HPO_4 and 100 NaCl (pH 7.4). All compounds ejected into the brain were dissolved in saline (NaCl 0.9%, pH 7.4). Ascorbate oxidase (AAOx) was obtained from AppliChem (Darmstadt, Germany) and was prepared by dissolving 0.1 mg (28.8 U) of the enzyme in 1.0 mL of saline. High K^+ solution was prepared in Milli-Q water and had the following composition (in mM): 70 KCl, 79 NaCl, 2.5 $CaCl_2$. Glutamate oxidase (US Biological, Swampscott, MA) was prepared by adding 50 μL of purified H_2O to the lyophilized, purified enzyme (25 units) to obtain a final concentration of 0.5 U/μL. Carbon nanotubes (SWCNT and MWCNT) were purchased from Nano-lab (USA) and they were suspended in a 0.5% Nafion solution to a final concentration of 100 mg/mL.

2.2. Electrochemical instrumentation

All recordings were performed using a FAST16mkII potentiostat system (Quanteon, LLC., USA). Electrochemical recordings were performed in a 2-electrode electrochemical cell configuration mode consisting of the ascorbate/glutamate sensor as a working electrode and an Ag/AgCl in 3 M KCl (RE-5B, BAS Inc.) as a reference electrode. For *in vivo* experiments, the reference was replaced by a miniature pseudo-reference electrode produced by electro-oxidation of the exposed tip of a Teflon-coated Ag wire (200 μm o.d., Science Products, Germany). The holding potential for the ascorbate nanocomposite sensor was +0.05 V *vs.* Ag/AgCl, based on the voltammetry studies shown in this work and according to the values previously reported [13]. In the case of the glutamate biosensor, the holding potential was +0.70 V *vs.* Ag/AgCl, as referred in the literature [19,24,25]. Data display rate was 2 Hz for all recordings.

2.3. Ascorbate microelectrode preparation and calibration

Carbon fiber microelectrodes were fabricated as previously described [26] and the exposed tip of the carbon fiber (o.d. 30 μm) was cut to a length of 150–250 μm. Single- and multi-wall carbon nanotubes (SWCNT and MWCNT, respectively) were used to coat the exposed surface of the CFMs. In each case, a single drop of the suspension was applied onto a glassy plate and the CFM tip was immersed into the droplet for 30 s and then dried at 170^{0}C for 5 min.

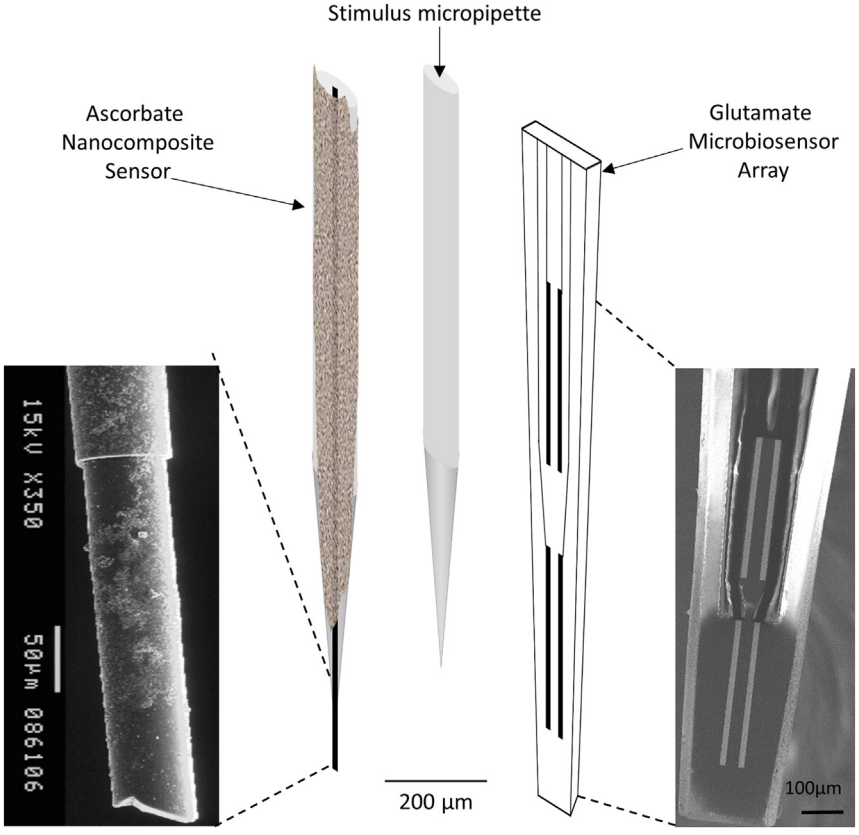

Fig. 1. Schematic representation of the array composed by the ascorbate nanocomposite microsensor (left), the glutamate microbiosensor (right) and the micropipette (center) used for local application of solutions in the extracellular space of the rat hippocampus.

Calibration was performed in PBS 0.05 M at room temperature (*ca.* 22 °C). Once a stable baseline was obtained, 3 successive additions of ascorbate (100 μM each) were followed by DA (20 μM) and NO_2^- (50 μM). Sensitivity, detection limit (LOD), linearity and selectivity were calculated from the data.

2.4. Glutamate microbiosensor arrays

Glutamate microbiosensor arrays were prepared using S2-type MEAs (Center for Microelectrode Technology, University of Kentucky, USA) consisting of 2 pairs of side-by-side Pt sites (15 × 333 μm) on a ceramic substrate (100 μm between pairs and 30 μm between sites in each pair). Their fabrication process is described elsewhere [20]. A 10-μL cocktail solution containing 1% glutamate oxidase (GluOx), 1% Bovine serum albumin (BSA) and 0.125% glutaraldehyde was prepared and used fresh. A microsyringe (Hamilton Co.) was used to manually coat the MEA recording sites with the enzyme solution under a stereomicroscope. A droplet of the solution (~0.1 μL) was suspended at the tip of the microsyringe and the solution was applied to the bottom pair of the recording sites for a 5-s period. This procedure was repeated 3 times, with a one-minute interval. The top pair of recording sites was coated in a similar manner using a protein matrix (1% BSA and 0.125% glutaraldehyde). The microbiosensor arrays were allowed a minimum 72 h curing period in a low-humidity environment at room temperature prior to use.

The 1,3-phenylenediamine (*m*-PD) was electropolymerized onto the Pt recording surfaces to create an exclusion layer and improve selectivity towards glutamate. Electropolymerization was performed in a degassed 5 mM solution of m-PD, by applying a triangular potential wave with an offset of +0.5 V, peak to peak amplitude equal to ± 0.25 V, at a frequency of 0.05 Hz, for a period of 20 min [27].

Glutamate microbiosensor arrays were calibrated in PBS 0.05 M at 37 °C. Once a stable baseline was obtained, a single addition of ascorbate (250 μM) was followed by 3 additions of L-glutamate (20 μM) and DA (20 μM). Finally, 20 μM of H_2O_2 was added to the beaker to check that the sites were responding to the reporter molecule. Sensitivity, LOD and linearity (R^2) for glutamate were calculated, as well as the selectivity ratio over ascorbate.

For *in vivo* simultaneous recording of ascorbate and glutamate, the micro(bio)sensors were coupled to a pulled micropipette (tip diameter *ca.* 10 μm) in an array, as depicted in Fig. 1. The micropipette used for the local application of stimulus solution was placed between the ascorbate CFM and the glutamate microbiosensor, at approximately 200 μm from each one. The distance between the three elements was controlled with the help of a microscope fitted with an eyepiece reticule, and the array was fixed with the use of sticky wax.

2.5. Animals and surgical procedures

All experiments were performed in accordance with the European Community Council Directive for the Care and Use of Laboratory Animals (2010/63/EU) and were approved by the local institutional animal care committee (ORBEA). In the present study, we used 6 adult male Wistar rats (8–12 weeks; weight between 250 and 300 g) maintained in a 12:12 light: dark cycle with food and water available *ad libitum*.

The experimental setup used for recording ascorbate/glutamate *in vivo* in anesthetized rats was similar to that used in previous studies [26]. Briefly, rats were anesthetized with urethane (1.25–1.50 g/kg, i.p.) and placed in a stereotaxic frame (Stoelting, USA). Body temperature was maintained at 37 °C using a delta phase isothermal pad (BrainTree Scientific, MA, USA). A craniotomy was performed to expose the brain area of interest. After removing the dura mater, the microsensor/biosensor/micropipette array was lowered into the rat hippocampus using pre-determined coordinates [28]. Specific coordinates used in each experiment are indicated in each figure legend. A miniature Ag/AgCl pseudo-reference electrode was placed beneath the exposed skin and soaked with a 0.9% NaCl solution during the experiments. Physiological conditions were recorded using a MouseOx oximeter (Starr Life Science, Allegheny Avenue Oakmont, PA, USA). After stabilization of baseline current (*ca.* 15 min), solutions were locally pressure ejected into the brain adjacent to the microelectrode/

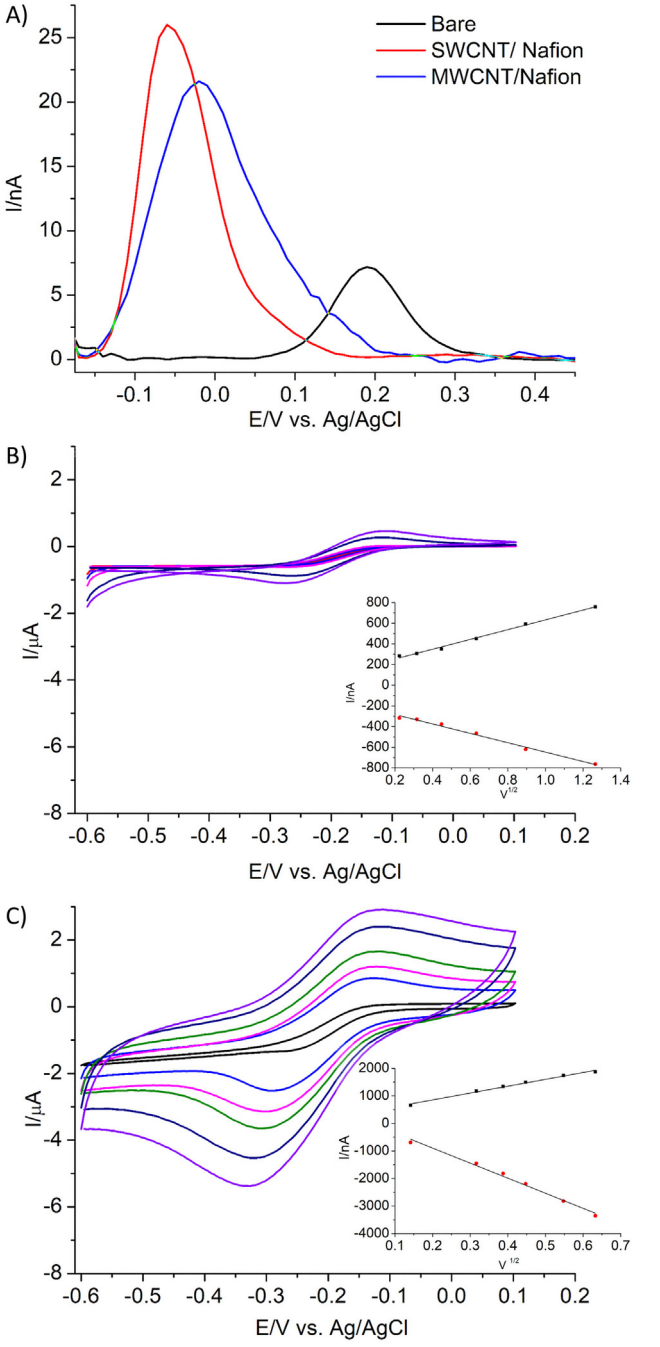

Fig. 2. A) Square wave voltammograms of ascorbate (500 μM) in PBS pH 7.4 obtained using a bare (black trace) and nanocomposite modified (red and blue traces) CFMs. Square wave voltammetry parameters: f = 10 Hz, E_{step} = 2 mV, E_{SW} = 10 mV. Determination of microelectrode active surface area of bare (B) and SWCNT/Nafion® modified (C) CFMs by cyclic voltammetry. Voltammograms obtained in hexaammineruthenium (III) chloride (5 mM) in 1 M KNO_3 at scan rates ranging from 20 to 1600 mV s^{-1}. Linear regression plots of the oxidation and reduction peak potentials for bare and SWCNT/Nafion® CFMs are shown inset and regression equations were the following: Bare CFMs: oxidation: y = 158.8 + 473.6x; r^2 = 0.993; reduction: y = −192.6 − 454.5x r^2 = 0.988 SWCNT/Nafion® CFMs: oxidation: y = 356.4 + 2488.5x; r^2 = 0.989, reduction: y = 200.5 − 5472.9x; r^2 = 0.996. (For interpretation of the references to color in this figure legend, the reader is referred to the web version of this article.)

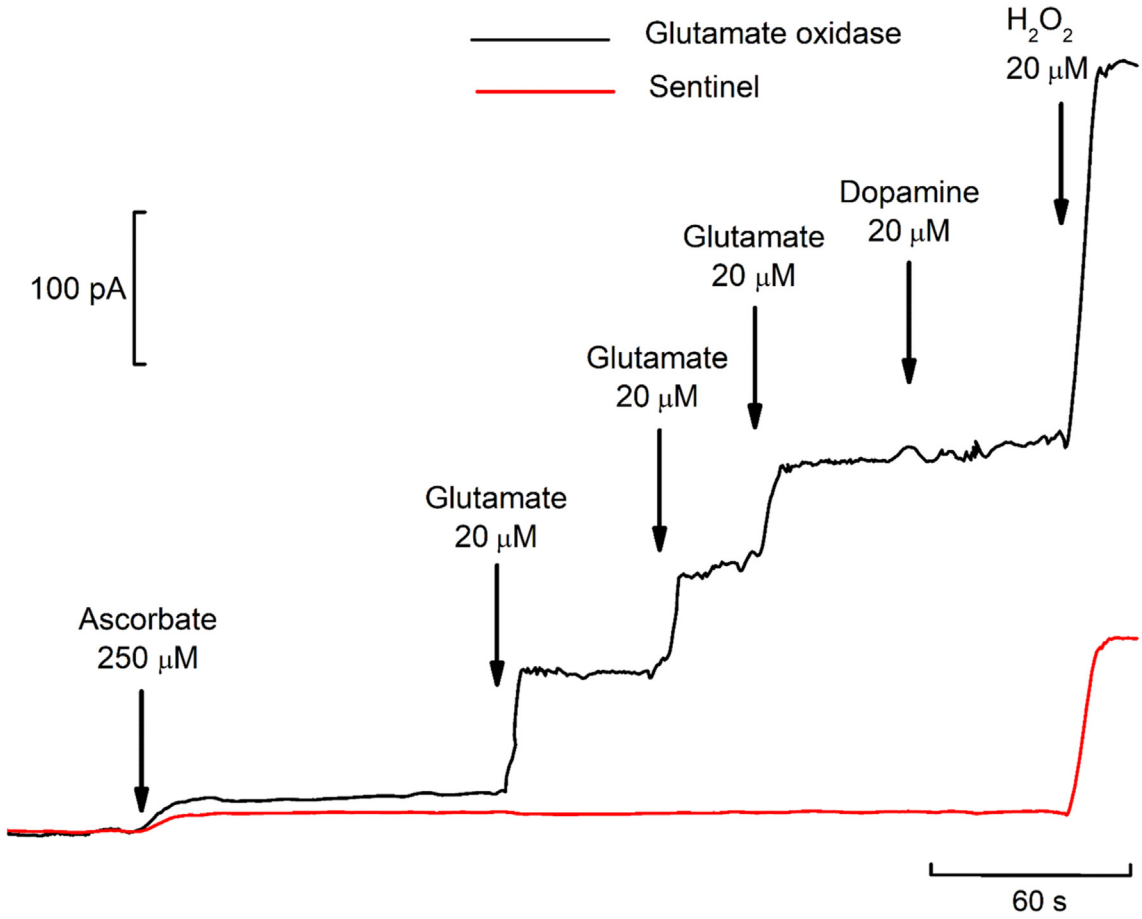

Fig. 3. Representative amperometric calibration of a glutamate microbiosensor array at +0.7 V *vs.* Ag/AgCl, showing one GluOx coated site (black trace) and one sentinel site (red trace). Three successive additions of a glutamate solution (20 μM) were performed in the presence of ascorbate (250 μM) followed by a single addition of dopamine (20 μM). At the end of the calibration the responsiveness of the microelectrode array recoding sites was tested by addition of H_2O_2 (20 μM). (For interpretation of the references to color in this figure legend, the reader is referred to the web version of this article.)

biosensor sites from the glass micropipette using a Picospritzer III (Parker Hannifin Corp., General Value, Fairfield, NJ, USA).

2.6. Data analysis

Data analysis was performed using OriginLab Pro 7.5 and GraphPad Prism 5. Data are presented as mean ± SEM. Differences between two data sets were evaluated by a Student's *t*-test. Statistical tests between multiple data sets were carried out using a one-way analysis of variance (ANOVA). Each glutamate signal obtained *in vivo* was analyzed to determine the following parameters: peak amplitude, rise time (T_R, the time from stimulus ejection to peak amplitude), and total signal duration (T_{Total}, the time from stimulus ejection until complete return to signal baseline) and uptake rate (μM s^{-1}), k^{-1} × maximum amplitude (where k^{-1} is the slope of the linear regression of the natural log transformation of the decay over time). The current signal was converted into glutamate concentration using calibration sensitivity obtained for each site.

3. Results and discussion

3.1. Ascorbate oxidation potential and electroactive surface area

The oxidation of ascorbate at bare carbon electrodes requires high over-potentials due to slow electron transfer kinetics. A two-electron oxidation reaction converts ascorbate into dehydroascorbic acid, which is rapidly hydrolyzed ($k = 1.2 \times 10^3$ s^{-1}) to 2,3-diketogulanic acid, a non-electroactive product that readily adsorbs onto the electrode surface [29,30]. However, the oxidation reaction of ascorbate on carbon electrodes undergoes an inner-sphere electron transfer and is sensitive to the nature of electrode surface, which can be fine-tuned by physical or chemical modifications such as the immobilization of CNTs. As shown in Fig. 2A, we observed a significant ($p < 0.05$) negative shift of the oxidation peak potential from +0.20 V *vs.* Ag/AgCl for bare CFMs to −0.05 V and to −0.02 V for SWCNT/Nafion® and MWCNT/Nafion® modified CFMs, respectively. This indicates an electrocatalytic effect in agreement with previous reports [13,31,32]. Given the similar electrocatalytic effect ($p > 0.05$) observed for both nanocomposite films and

Table 1
Analytical and kinetic parameters obtained for the glutamate microbiosensor array. Values are shown as mean ± SEM.

Sensitivity (pA μM^{-1})	Linearity (R^2)	Response time $t_{50\%}$ (s)	LOD (nM)	Selectivity ratio		Vmax (nA)	K_M (μM)
				Dopamine	Ascorbate		
5.3 ± 0.8 (n = 18)	0.998 ± 0.001 (n = 18)	0.9 ± 0.02 (n = 6)	204 ± 32 (n = 10)	438 ± 178 (n = 6)	404 ± 84 (n = 6)	8.3 ± 0.5 (n = 4)	592 ± 114 (n = 4)

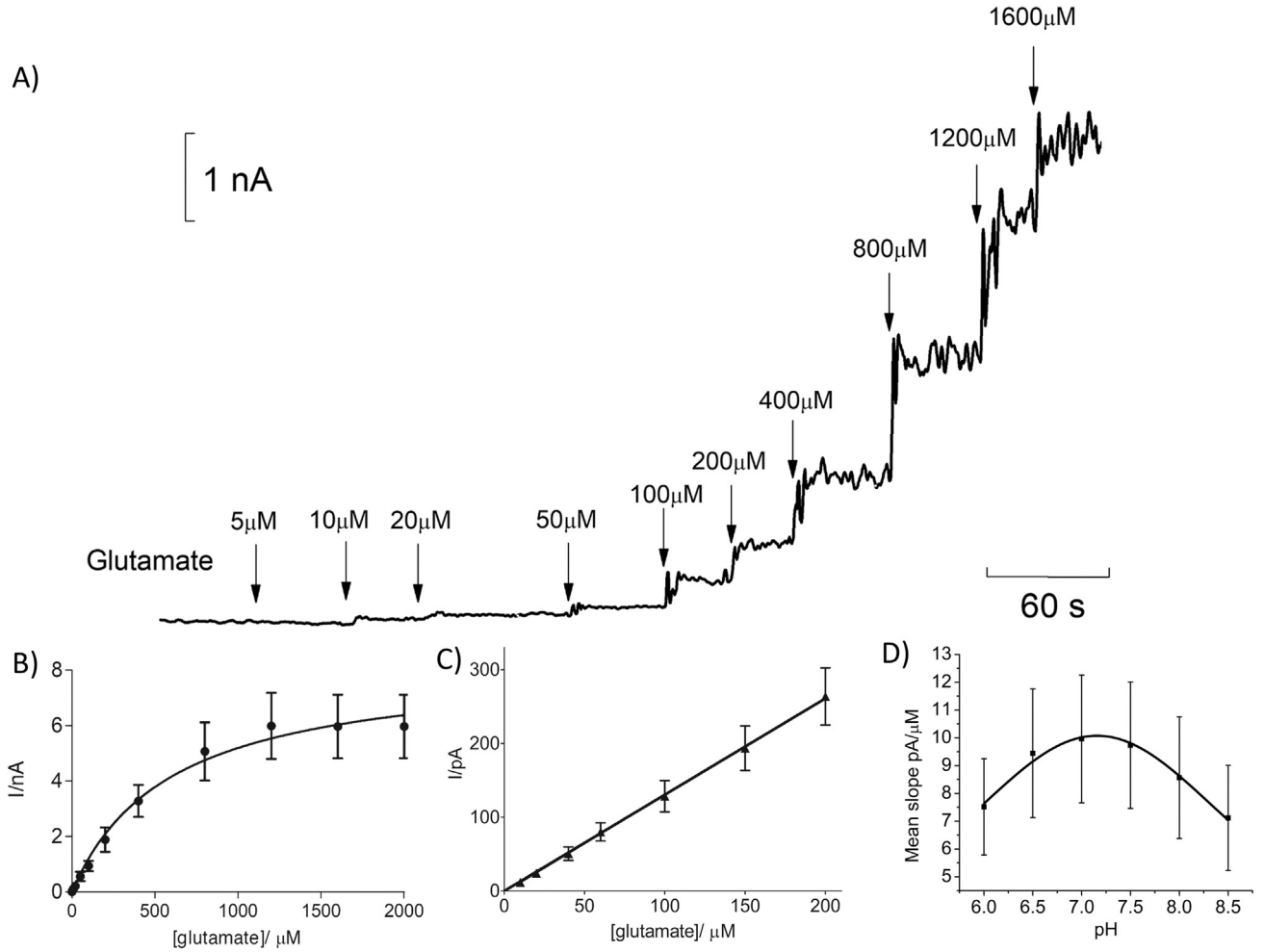

Fig. 4. Determination of enzyme kinetics for the glutamate microbiosensor array. A) Representative calibration recording between 5 and 1600 μM glutamate. B) Calibration plot of steady-state current as a function of glutamate concentration. Data was fitted to a Michaelis-Menten equation (n = 6). C) Calibration plot showing the linear range between 2 and 200 μM glutamate (n = 6). D) Effect of pH on the microbiosensor performance. The slope of the calibration curve is plotted as a function of pH and data was fitted to a Gaussian function (n = 4).

that we have previously reported an increase in the sensitivity resulting from the modification of CFMs with SWCNT/Nafion® [13] we selected this nanocomposite for *in vivo* experiments.

To assess whether an increase in the electroactive surface area may underlie the enhanced sensitivity, we used a standard redox couple to evaluate the electrochemical behavior of bare and SWCNT/Nafion® CFMs. Cyclic voltammograms were recorded in a solution of hexaammineruthenium (III) chloride (5 mM) in 1 M KNO_3 at scan rates ranging from 20 to 1600 mV s^{-1}. As shown in the insets of Fig. 2B and C, the anodic (black trace) and cathodic (red trace) peak currents increased linearly with the square root of the scan rate for bare and CNT-modified CFMs, indicating that the process is diffusion controlled. The electroactive surface area of each type of CFMs, calculated using the Randles-Sevcik equation was calculated to be $1.4 \pm 0.2 \times 10^{-4}$ cm^2 and $16.0 \pm 2.2 \times 10^{-4}$ cm^2 for bare CFMs and SWCNT/Nafion® modified CFMs, respectively (c.a. 10-fold increase).

3.2. Analytical performance of the glutamate microbiosensor array

The analytical performance of the glutamate microbiosensor array was evaluated *in vitro* to validate its use *in vivo*. Fig. 3 shows a typical calibration recording of a S2 type MEA glutamate microbiosensor. For each calibration, the sensitivity, LOD, linearity and selectivity towards ascorbate and DA were calculated as summarized in Table 1. Values are in good agreement with those previously reported [19,20].

Considering that in the extracellular space, the concentration of glutamate is typically in the low micromolar range [21] and the high K_M values of the enzyme GluOx (0.3 to 5 mM) [33], little concern is usually paid to the kinetic parameters K_M and V_{max}. However, enzyme load on the microelectrode may have a significant impact on efficiency [34], more so given that GluOx is applied manually onto the MEA surface. We performed a calibration of the glutamate microbiosensor between the concentration range of 5 to 1600 μM (Fig. 4A) and fitted the data to a Michaelis-Menten nonlinear fit (Fig. 4B) in order to calculate K_M and V_{max}, as summarized in Table 1. It is also important to note that the microbiosensor arrays exhibited a linear response in the range of 1 to 200 μM glutamate.

Table 2
Evaluation of glutamate transient signals obtained from local application of KCl and glutamate in the CA1-region of the rat hippocampus. Values are shown as mean ± SEM.

	Hippocampus (CA1)	
	KCl 70 mM	Glutamate 20 mM
Number of rats	3	3
Number of signals	22	17
Maximum peak amplitude (μM)	9.6 ± 1.4	39.3 ± 8.4
T_{rise} (s)	3.0 ± 0.3	3.8 ± 0.2
T_{total} (s)	10.6 ± 0.7	21.3 ± 2.2
Uptake rate (μM s^{-1})	3.2 ± 1.0	5.8 ± 1.1

We further determined the dependency of the microbiosensor response (calculated as the slope of the calibration curve) on pH (Fig. 4D). The microbiosensor response showed a bell-shaped curve between pH 6.0 to 8.5. The response to glutamate was fitted to a Gaussian function and optimal activity peaked at pH 7.20 ± 0.04 ($r^2 = 0.96$; n = 4), which is close to physiological pH *in vivo*. Oxygen is a co-substrate in the reaction catalyzed by GluOx. Reports indicate that glutamate biosensors are minimally affected by O_2 concentration [22]. This low dependency may be related with the triple coating of the Pt surface with GluOx that leads to an increase of the enzyme load and decreased O_2 dependency of the biosensor [35]. Also, a portion of O_2 is returned to the tissue by the oxidation of H_2O_2 at the MEA surface, minimizing the influence of O_2 concentration on glutamate responses. It was previously reported that the GluOx biosensor response at an O_2 concentration of 30 μM was within 75% of that obtained in air-saturated buffer [36]. Considering the low concentrations of glutamate present in the central nervous system [22,37], one may expect little O_2-dependency.

The analytical performance of the glutamate biosensor was evaluated *in vivo* in the hippocampus (CA1 subregion) of anesthetized rats. We evaluated the transient glutamate signals produced upon K^+-induced depolarization and exogenous application of glutamate. As can be observed in Fig. S1, local applications of high-K^+ solution (25–60 nL) produced transient and reproducible increases in extracellular levels of glutamate. Exogenously applied glutamate solution (20 mM, 12.5–75 nL) also produced transient increases in extracellular glutamate *in vivo* (not shown). The amperometric signals were characterized and results are presented in Table 2. As expected, the peak amplitude for 20 mM glutamate ejections was higher when compared with 70 mM KCl stimulation, which produces endogenous release of glutamate due to K^+-evoked depolarization. The average uptake rate of glutamate, calculated by fitting the signal decrease phase to a first-order exponential decay function, was 5.8 μM s^{-1} for exogenous glutamate and 3.2 μM s^{-1} ($p > 0.05$, Student's *t*-test) for KCl-evoked endogenously released glutamate, confirming previous reports of fast glutamate clearance from the extracellular space [38].

It is important to mention that these glutamate microbiosensor arrays allow recording in a "self-referencing" mode. Two of the identical 4 Pt recording sites were used as sentinel or null sites since they are coated with a protein matrix not containing GluOx. As shown in Fig. 3, these sites respond to interferents such as ascorbate in a similar fashion as the GluOx coated sites, but show no response to glutamate. Subtraction of the signal recorded at the sentinel site from that recorded at the GluOx coated sites (as shown in Fig. S2) not only improves signal selectivity, but also improves the signal-to-noise ratio and LOD. The self-referencing technique allows cross-checking for interferent signals on a moment-to-moment basis.

3.3. In vivo basal ascorbate levels in the rat hippocampus

Prior to *in vivo* use, each nanocomposite CFM was calibrated in 0.05 M PBS at room temperature to access sensitivity, LOD and selectivity relative to DA and NO_2^-. On average, the sensitivity was 42 pA μM^{-1} (n = 7) and LOD was 0.7 μM. Furthermore, no detectable response was observed for DA (20 μM) or NO_2^- (50 μM). We used these SWCNT/Nafion® modified CFMs to estimate basal ascorbate levels *in vivo* in the CA1, CA3 and DG sub-regions of the hippocampus of urethane-anesthetized rats. To this purpose, we determined the change in signal following removal of ascorbate by local ejection of AAOx in each subregion of the hippocampus (Fig. 5). The current change was converted to ascorbate concentration according to post-calibration sensitivity. Resting ascorbate levels in the different hippocampus sub-regions were, thus, determined to be 276 ± 60 μM (n = 10) in CA1, 183 ± 30

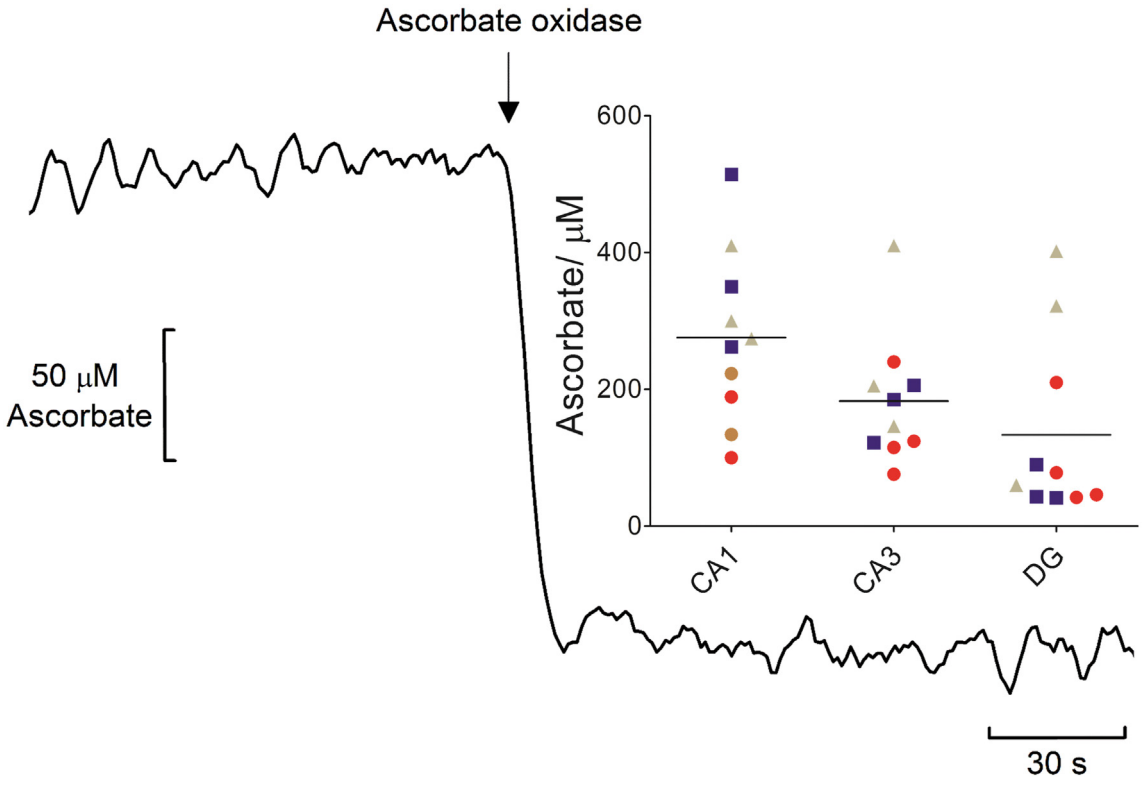

Fig. 5. Representative *in vivo* amperometric recording for estimation of resting ascorbate level in the CA1 hippocampal sub-region of urethane-anesthetized rat. Ascorbate oxidase (50 nL; 0.1 mg/mL) was applied locally to deplete extracellular ascorbate. The change in current following AAOx pressure-ejection was used to estimate resting levels of ascorbate (μM) in the sub-regions of the rat hippocampus. The inset shows values obtained from three different rats, each represented by a different color and symbol. Horizontal line represents mean value (n = 10).

μM (n = 10) in CA3 and 133 ± 42 μM (n = 10) in DG. Values reported in the literature usually refer to the hippocampus as a whole [39] and are in line with the average concentration we found considering the three sub-regions here analyzed (*ca.* 200 μM).

3.4. Simultaneous and real-time in vivo measurement of glutamate and ascorbate

To further understand the interplay between ascorbate and glutamate in the hippocampus, we performed simultaneous *in vivo* recordings of the two compounds in the CA1 subregion of the hippocampus of urethane-anesthetized rats. For this purpose, we assembled a SWCNT/Nafion® modified CFM sensor and glutamate microbiosensor array alongside with a glass micropipette for local pressure-ejection of KCl 70 mM or glutamate 20 mM (see Fig. 1). As shown in Fig. 6 A and B, both stimuli produced transient increases in glutamate followed (*ca.* 1 s delay) by an increase in ascorbate. The ascorbate signal peaked when the glutamate peak ended. Furthermore, Fig. 6A indicates that for a glutamate peak of *ca.* 6 μM, ascorbate peaked at *ca.* 100 μM. Recordings shown in Fig. 6B indicate a maximum glutamate peak of *ca.* 65 μM and *ca.* 400–500 μM of ascorbate. This result suggests that there is a correlation between the peak amplitude and concentration of glutamate and ascorbate in the extracellular space.

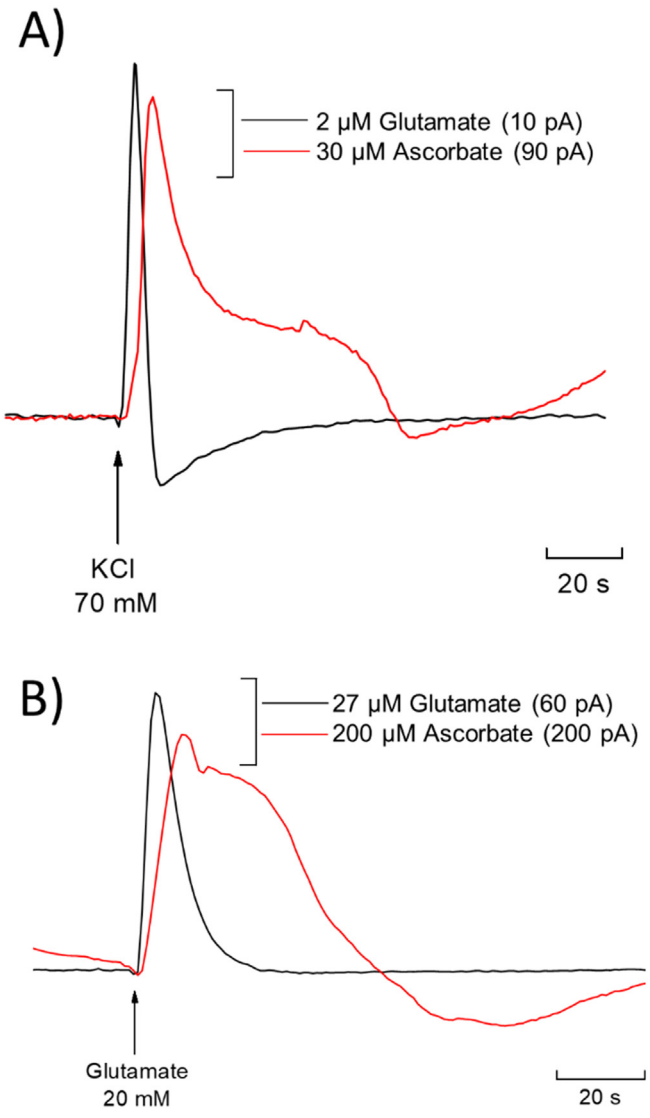

Fig. 6. Simultaneous *in vivo* amperometric recordings of glutamate (black trace) and ascorbate (red trace). (A) Nanocomposite sensor and glutamate microbiosensor array was implanted in the CA1 sub-region of the rat hippocampus (coordinates: AP −3.8 mm; ML −2.2 mm; DV −2.6 mm). Endogenous glutamate release was evoked by a local application of 25 nL KCl 70 mM. (B) Amperometric recordings in the DG sub-region (coordinates: AP −3.8 mm; ML −2.2 mm; DV −3.2 mm) during local application of glutamate (25 nL, 20 mM). Arrows indicate the pressure-ejection of each stimulus. (For interpretation of the references to color in this figure legend, the reader is referred to the web version of this article.)

Given the chemical complexity of the brain extracellular milieu, it is important to confirm the chemical identity of the ascorbate signals measured. The negative shift in the oxidation potential of ascorbate observed at the SWCNT/Nafion®-modified CFM suggest a high selectivity of the nanocomposite sensor against major interferents found in the brain extracellular space such as dopamine and other catecholamines [13]. Nonetheless, we confirmed the chemical identity of the amperometric signal measured *in vivo* by obtaining successive square wave voltammograms during the experiment. As shown in the false color plot in Fig. 7, local application of a bolus of 20 mM glutamate produced a transient increase in current at the oxidation peak potential of ascorbate and with a time frame similar to the signals recorded by amperometry for the same stimulus conditions (Fig. 6B).

In vivo biofouling may occur due to adsorption of macromolecules and tissue inflammatory response and has been reported to decrease sensitivity by 60 to 82% of the initial value [13,40]. To evaluate the extent of biofouling at the nanocomposite sensor, we performed local injections of exogenous ascorbate (20 mM) at 400 s, 2309 s and 6480 s after insertion the microsensor into the brain tissue and we found no significant change in measured peak amplitude, as shown in Fig. S3. The results support the reliability of the post-calibration data and demonstrate a high stability of the sensitivity of the nanocomposite CFM during *in vivo* experiments.

Overall, the results corroborate previous data indicating an interplay between ascorbate and glutamate [39,41], putatively *via* a heteroexchange mechanism [41,42]. The coupling between neuronal production of $^{\bullet}NO$ following glutamatergic stimulation and the release of ascorbate into the extracellular fluid, further supports the role of ascorbate in the modulation of glutamatergic signaling in the brain [2].

4. Conclusions

In the present work we demonstrated that CNT/Nafion® modified CFMs - nanocomposite sensors - display electrocatalytic properties towards the oxidation of ascorbate that translated into a negative shift in oxidation potential and a significant increase in the electroactive surface area. Furthermore, they revealed suitable recording properties *in vivo*, such as selectivity, stable sensitivity and minimal biofouling. Using these nanocomposite sensors, we estimated the *in vivo* basal ascorbate levels in the sub-regions of the rat hippocampus.

Ceramic-based Pt microelectrode arrays coated with glutamate oxidase were used to selectively monitor potassium-evoked glutamate release and reuptake in the rat hippocampus with high spatial and temporal resolution.

Finally, combination of the two micro(bio)sensors in an array allowed real-time and simultaneous measurements of glutamate and ascorbate *in vivo* in the hippocampus of anesthetized rats upon K^+ stimulus, revealing rapid concentration changes of these two neuroactive molecules following. Considering the recognized interplay between glutamate signaling and fluctuations in extracellular ascorbate levels and their putative role in brain pathophysiology, namely in age-related neurodegenerative diseases, the development of sensors which allow simultaneous *in vivo* measurements with high spatiotemporal resolution is highly relevant.

Acknowledgments

This work was funded by the European Regional Development Fund (ERDF), through the Centro 2020 Regional Operational Program: project

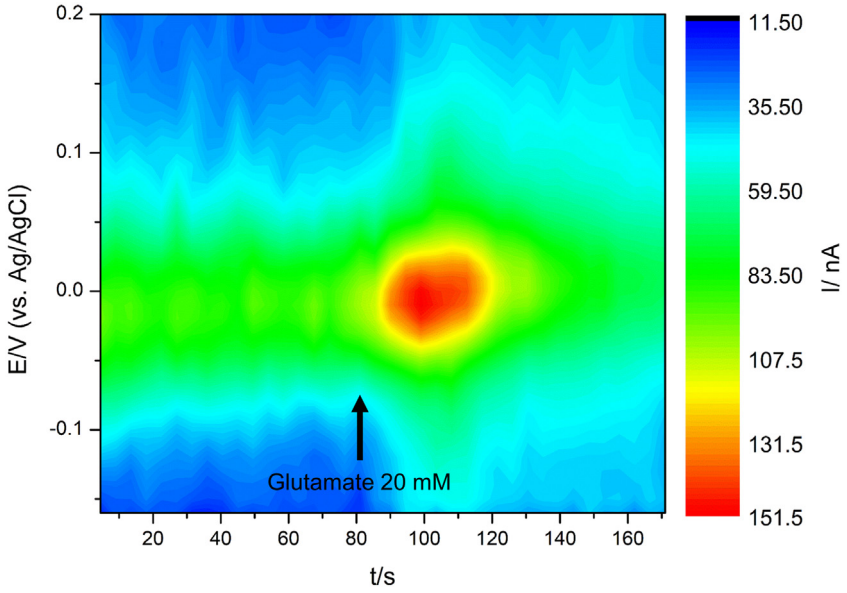

Fig. 7. False color plot of *in vivo* square wave voltammograms obtained with ascorbate nanocomposite sensor during a local ejection of glutamate 20 mM (indicated by the arrow) in the CA1 region of the rat hippocampus. The plot shows current intensity (false color) at each applied potential as a function of time. SWV parameters: $f = 50$ Hz, $E_{step} = 2$ mV, $E_{sw} = 10$ mV. (For interpretation of the references to color in this figure legend, the reader is referred to the web version of this article.)

CENTRO-01-0145-FEDER-000012-HealthyAging2020, the COMPETE 2020 - Operational Program for Competitiveness and Internationalization, and the Portuguese national funds *via* FCT – Fundação para a Ciência e a Tecnologia, I.P.: project POCI-01-0145-FEDER-007440.

Conflict of interest

GAG is the owner of Quanteon, LLC, which produces and sells the FAST16 recording system that was used for the *in vivo* measurements. GAG also designed the MEAs, which are distributed and sold by the Center for Microelectrode Technology (CeMeT) at the University of Kentucky. The other authors declare that they have no conflicts of interest.

Final disclosure

Nuno R. Ferreira contributed for:

1) The conception and design of the study, acquisition, analysis and interpretation of data;
2) Drafting the article and revising it critically for important intellectual content;
3) Final approval of the submitted version.

Ana Ledo contributed for:

1) The acquisition, analysis and interpretation of data relative to the *in vitro* evaluation of glutamate microbiosensors;
2) Drafting the article and revising it critically for important intellectual content;
3) Final approval of the submitted version.

João Laranjinha, contributed for:

1) Revising the article critically for important intellectual content;
2) Final approval of the version to be submitted.

Greg A. Gerhardt, contributed for:

1) Revising the article critically for important intellectual content;
2) Final approval of the submitted version.

Rui M. Barbosa, contributed for:

1) The conception and design of the study and interpretation of data;
2) Revising the article critically for important intellectual content;
3) Final approval of the submitted version.

Appendix A. Supplementary data

Supplementary data to this article can be found online at https://doi.org/10.1016/j.bioelechem.2018.01.009.

References

[1] R. Figueroa-Mendez, S. Rivas-Arancibia, Vitamin C in health and disease: its role in the metabolism of cells and redox state in the brain, Front. Physiol. 6 (2015), 397. https://doi.org/10.3389/fphys.2015.00397.
[2] N.R. Ferreira, C.F. Lourenco, R.M. Barbosa, J. Laranjinha, Coupling of ascorbate and nitric oxide dynamics in vivo in the rat hippocampus upon glutamatergic neuronal stimulation: a novel functional interplay, Brain Res. Bull. 114 (2015) 13–19, https://doi.org/10.1016/j.brainresbull.2015.03.002.
[3] J. Frade, S. Pope, M. Schmidt, R. Dringen, R. Barbosa, J. Pocock, J. Laranjinha, S. Heales, Glutamate induces release of glutathione from cultured rat astrocytes—a possible neuroprotective mechanism? J. Neurochem. 105 (4) (2008) 1144–1152, https://doi.org/10.1111/j.1471-4159.2008.05216.x.
[4] R.D. O'Neill, M. Fillenz, L. Sundstrom, J.N. Rawlins, Voltammetrically monitored brain ascorbate as an index of excitatory amino acid release in the unrestrained rat, Neurosci. Lett. 52 (3) (1984) 227–233.
[5] M. Miele, M.G. Boutelle, M. Fillenz, The physiologically induced release of ascorbate in rat brain is dependent on impulse traffic, calcium influx and glutamate uptake, Neuroscience 62 (1) (1994) 87–91.
[6] N.C. Danbolt, Glutamate uptake, Prog. Neurobiol. 65 (1) (2001) 1–105 (doi:S0301-0082(00)00067-8 [pii]).
[7] F.E. Harrison, G.L. Bowman, M.C. Polidori, Ascorbic acid and the brain: rationale for the use against cognitive decline, Nutrients 6 (4) (2014) 1752–1781, https://doi.org/10.3390/nu6041752.
[8] G.V. Rebec, From Interferant anion to neuromodulator: ascorbate oxidizes its way to respectability, Electrochemical Methods for Neurscience, CRC Press, Boca Raton (FL), 2007 doi:NBK2569 [bookaccession].
[9] G.V. Rebec, S.J. Barton, A.M. Marseilles, K. Collins, Ascorbate treatment attenuates the Huntington behavioral phenotype in mice, Neuroreport 14 (9) (2003) 1263–1265, https://doi.org/10.1097/01.wnr.0000081868.45938.12.
[10] M.L. Huffman, B.J. Venton, Carbon-fiber microelectrodes for in vivo applications, Analyst 134 (1) (2009) 18–24, https://doi.org/10.1039/b807563h.
[11] A.K. Sarma, P. Vatsyayan, P. Goswami, S.D. Minteer, Recent advances in material science for developing enzyme electrodes, Biosens. Bioelectron. 24 (8) (2009) 2313–2322 doi:S0956-5663(08)00561-7 [pii] https://doi.org/10.1016/j.bios.2008.09.026.

[12] L. Agui, P. Yanez-Sedeno, J.M. Pingarron, Role of carbon nanotubes in electroanalytical chemistry: a review, Anal. Chim. Acta 622 (1–2) (2008) 11–47 doi:S0003-2670(08)00999-9 [pii] https://doi.org/10.1016/j.aca.2008.05.070.
[13] N.R. Ferreira, R.M. Santos, J. Laranjinha, R.M. Barbosa, Real time in vivo measurement of ascorbate in the brain using carbon nanotube-modified microelectrodes, Electroanalysis 25 (7) (2013) 1757–1763, https://doi.org/10.1002/elan.201300053.
[14] T.X. Hanjun Cheng, Dalei Wang, Jie Hao, Yu Ping, Lanqun Mao, Simultaneous in vivo ascorbate and electrophysiological recordings in rat brain following ischemia/reperfusion, J. Electroanal. Chem. 781 (2016) 90–96, https://doi.org/10.1016/j.jelechem.2016.10.024.
[15] W. Timmerman, B.H. Westerink, Brain microdialysis of GABA and glutamate: what does it signify? Synapse 27 (3) (1997) 242–261, https://doi.org/10.1002/(SICI)1098-2396(199711)27:3<242::AID-SYN9>3.0.CO;2-D.
[16] K.L. Clapp-Lilly, R.C. Roberts, L.K. Duffy, K.P. Irons, Y. Hu, K.L. Drew, An ultrastructural analysis of tissue surrounding a microdialysis probe, J. Neurosci. Methods 90 (2) (1999) 129–142.
[17] E.R. Hascup, S. AFBjerken, K.N. Hascup, F. Pomerleau, P. Huettl, I. Stromberg, G.A. Gerhardt, Histological studies of the effects of chronic implantation of ceramic-based microelectrode arrays and microdialysis probes in rat prefrontal cortex, Brain Res. 1291 (2009) 12–20, https://doi.org/10.1016/j.brainres.2009.06.084.
[18] K.N. Hascup, E.R. Hascup, Electrochemical techniques for subsecond neurotransmitter detection in live rodents, Comp. Med. 64 (4) (2014) 249–255.
[19] J.J. Burmeister, G.A. Gerhardt, Self-referencing ceramic-based multisite microelectrodes for the detection and elimination of interferences from the measurement of L-glutamate and other analytes, Anal. Chem. 73 (5) (2001) 1037–1042.
[20] J.J. Burmeister, K. Moxon, G.A. Gerhardt, Ceramic-based multisite microelectrodes for electrochemical recordings, Anal. Chem. 72 (1) (2000) 187–192.
[21] B.K. Day, F. Pomerleau, J.J. Burmeister, P. Huettl, G.A. Gerhardt, Microelectrode array studies of basal and potassium-evoked release of L-glutamate in the anesthetized rat brain, J. Neurochem. 96 (6) (2006) 1626–1635, https://doi.org/10.1111/j.1471-4159.2006.03673.x.
[22] J.M. Hinzman, T.C. Thomas, J.J. Burmeister, J.E. Quintero, P. Huettl, F. Pomerleau, G.A. Gerhardt, J. Lifshitz, Diffuse brain injury elevates tonic glutamate levels and potassium-evoked glutamate release in discrete brain regions at two days post-injury: an enzyme-based microelectrode array study, J. Neurotrauma 27 (5) (2010) 889–899, https://doi.org/10.1089/neu.2009.1238.
[23] E.C. Rutherford, F. Pomerleau, P. Huettl, I. Strömberg, G.A. Gerhardt, Chronic second-by-second measures of l-glutamate in the central nervous system of freely moving rats, J. Neurochem. 102 (3) (2007) 712–722.
[24] J.J. Burmeister, F. Pomerleau, M. Palmer, B.K. Day, P. Huettl, G.A. Gerhardt, Improved ceramic-based multisite microelectrode for rapid measurements of L-glutamate in the CNS, J. Neurosci. Methods 119 (2) (2002) 163–171 (doi:S0165027002001723 [pii]).
[25] F. Pomerleau, B.K. Day, P. Huettl, J.J. Burmeister, G.A. Gerhardt, Real time in vivo measures of L-glutamate in the rat central nervous system using ceramic-based multisite microelectrode arrays, Ann. N. Y. Acad. Sci. 1003 (2003) 454–457.
[26] R.M. Barbosa, C.F. Lourenco, R.M. Santos, F. Pomerleau, P. Huettl, G.A. Gerhardt, J. Laranjinha, In vivo real-time measurement of nitric oxide in anesthetized rat brain, Methods Enzymol. 441 (2008) 351–367 doi:S0076-6879(08)01220-2 [pii] https://doi.org/10.1016/S0076-6879(08)01220-2.
[27] N. Kevin, E.C.R. Hascup, E. Jorge, B. Keith Day Quintero, Justin R. Nickell, Francois Pomerleau, Peter Huettl, Jason J. Burmeister, Greg A. Gerhardt, Second-by-second measures of L-glutamate and other neurotransmitters using enzyme-based microelectrode arrays, in: Adrian C. Michael LMB (Ed.), Electrochemical Methods for Neuroscience, Taylor & Francis Group, Boca Raton 2006, pp. 407–450.
[28] C.P.G. Watson, The Rat Brain in Stereotaxic Coordinates, 6th Edition, 6th edn Elsevier Inc., 2007
[29] C.R. Raj, T. Ohsaka, Electroanalysis of ascorbate and dopamine at a gold electrode modified with a positively charged self-assembled monolayer, J. Electroanal. Chem. 496 (1–2) (2001) 44–49, https://doi.org/10.1016/S0022-0728(00)00335-1.
[30] A. Liu, I. Honma, H. Zhou, Simultaneous voltammetric detection of dopamine and uric acid at their physiological level in the presence of ascorbic acid using poly(-acrylic acid)-multiwalled carbon-nanotube composite-covered glassy-carbon electrode, Biosens. Bioelectron. 23 (1) (2007) 74–80, https://doi.org/10.1016/j.bios.2007.03.019.
[31] Y.F. Zhao, Y.Q. Gao, D.P. Zhan, H. Liu, Q. Zhao, Y. Kou, Y.H. Shao, M.X. Li, Q.K. Zhuang, Z.W. Zhu, Selective detection of dopamine in the presence of ascorbic acid and uric acid by a carbon nanotubes-ionic liquid gel modified electrode, Talanta 66 (1) (2005) 51–57, https://doi.org/10.1016/j.talanta.2004.09.019.
[32] S.B. Hocevar, J. Wang, R.P. Deo, M. Musameh, B. Ogorevc, Carbon nanotube modified microelectrode for enhanced voltammetric detection of dopamine in the presence of ascorbate, Electroanalysis 17 (5–6) (2005) 417–422, https://doi.org/10.1002/elan.200403175.
[33] System B-TcEI, Information on EC 1.4.3.11 - L-glutamate oxidase, http://www.brenda-enzymes.org/enzyme.php?ecno=1.4.3.11 2015 2015.
[34] C.P. McMahon, G. Rocchitta, P.A. Serra, S.M. Kirwan, J.P. Lowry, R.D. O'Neill, The efficiency of immobilised glutamate oxidase decreases with surface enzyme loading: an electrostatic effect, and reversal by a polycation significantly enhances biosensor sensitivity, Analyst 131 (1) (2006) 68–72, https://doi.org/10.1039/b511643k.
[35] C.P. McMahon, G. Rocchitta, P.A. Serra, S.M. Kirwan, J.P. Lowry, R.D. O'Neill, Control of the oxygen dependence of an implantable polymer/enzyme composite biosensor for glutamate, Anal. Chem. 78 (7) (2006) 2352–2359, https://doi.org/10.1021/ac0518194.
[36] J.J. Burmeister, T.D. Coates, G.A. Gerhardt, Multisite microelectrode arrays for measurements of multiple neurochemicals, Conference Proceedings: Annual International Conference of the IEEE Engineering in Medicine and Biology Society IEEE Engineering in Medicine and Biology Society Annual Conference, 7, 2004, pp. 5348–5351, https://doi.org/10.1109/IEMBS.2004.1404493.
[37] F. Tian, A.V. Gourine, R.T. Huckstepp, N. Dale, A microelectrode biosensor for real time monitoring of L-glutamate release, Anal. Chim. Acta 645 (1–2) (2009) 86–91, https://doi.org/10.1016/j.aca.2009.04.048.
[38] J.E. Quintero, B.K. Day, Z. Zhang, R. Grondin, M.L. Stephens, P. Huettl, F. Pomerleau, D.M. Gash, G.A. Gerhardt, Amperometric measures of age-related changes in glutamate regulation in the cortex of rhesus monkeys, Exp. Neurol. 208 (2) (2007) 238–246, https://doi.org/10.1016/j.expneurol.2007.08.002.
[39] B. Ghasemzadeh, J. Cammack, R.N. Adams, Dynamic changes in extracellular fluid ascorbic acid monitored by in vivo electrochemistry, Brain Res. 547 (1) (1991) 162–166.
[40] M. Zhang, K. Liu, L. Xiang, Y. Lin, L. Su, L. Mao, Carbon nanotube-modified carbon fiber microelectrodes for in vivo voltammetric measurement of ascorbic acid in rat brain, Anal. Chem. 79 (17) (2007) 6559–6565, https://doi.org/10.1021/ac0705871.
[41] K.H. Milby, I.N. Mefford, W. Chey, R.N. Adams, In vitro and in vivo depolarization coupled efflux of ascorbic acid in rat brain preparations, Brain Res. Bull. 7 (3) (1981) 237–242.
[42] R.A. Grunewald, M. Fillenz, Release of ascorbate from a synaptosomal fraction of rat brain, Neurochem. Int. 6 (4) (1984) 491–500 (doi:0197-0186(84)90120-7 [pii]).